IEEE Access
Multidisciplinary | Rapid Review | Open Access Journal

SPECIAL SECTION ON ADDRESSING CHALLENGING ISSUES OF GRIDS WITH HIGH PENETRATION OF GRID CONNECTED POWER CONVERTERS: TOWARDS FUTURE AND SMART GRIDS

Received June 30, 2020, accepted July 9, 2020, date of publication July 17, 2020, date of current version July 29, 2020.

Digital Object Identifier 10.1109/ACCESS.2020.3010068

Development of Fractional Order Modeling of Voltage Source Converters

MONIKA SHARMA[1], (Member, IEEE),
BHARAT SINGH RAJPUROHIT[1], (Senior Member, IEEE),
SAMAR AGNIHOTRI[1], (Member, IEEE), AND
AKSHAY KUMAR RATHORE[2], (Senior Member, IEEE)

[1]School of Computing and Electrical Engineering, Indian Institute of Technology Mandi, Mandi 175005, India
[2]Department of Electrical and Computer Engineering, Concordia University, Montreal, QC H3G 1M8, Canada

Corresponding author: Monika Sharma (monika_sharma@students.iitmandi.ac.in)

This work was supported by the Department of Science and Technology India-Fund for Improvement of Science and Technology (DST-FIST).

ABSTRACT This paper proposes a mathematical fractional order modelling of Voltage Source Converters (VSC). Fractional behaviour helps to model and describe a real object more accurately than the integer order model. State-space equations of VSC is obtained using fractional calculus in d-q domain. The Caputo derivative method is employed to eliminate complex definitions of fractional calculus and to get approximate solution with optimal design of parameters. A detailed analysis is performed on developed mathematical fractional order model of VSC including small-signal analysis and DC analysis. The stability and time-domain transient analysis is carried out to validate the fractional order VSC for its application as Distribution STATtic COMpensator (DSTATCOM) in power distribution system, using real-time simulator. Fractional-order capacitor and inductor are designed and modelled for verification of fractional order VSC through simulations. The real-time simulation results verify the effectiveness of proposed model. It shows that fractional order model can describe the operating characteristics of VSC more accurately. The comparative performance analysis demonstrates superior transient response in case of fractional order devices as compared to integer order.

INDEX TERMS DSTATCOM, fractional calculus, real-time simulator, small-signal analysis, voltage source converter.

NOMENCLATURE

ω	Constant velocity
C_{dc}	dc link capacitor
I_{dc}	Current across capacitor
I_{load}	Load current
I_{shunt}	Shunt current
L_{shunt}	Shunt inductance
L_{source}	Inductance at source end
PCC	Point of Common Coupling
R_{load}	Load resistance
R_{shunt}	Shunt resistance
R_{source}	Resistance at source end of grid
V_{dc}	dc link voltage
V_{inp}	Input voltage at PCC
V_{VSC}	Voltage across voltage source converter

The associate editor coordinating the review of this manuscript and approving it for publication was Dinesh Kumar.

I. INTRODUCTION

In nature, all the systems have certain fractional characteristics. The concepts of fractional calculus has recently been applied to large number of linear and non-linear systems. Fractional calculus was considered earlier only a theoretical approach, but since last decade this technique has emerged as a better practical approach. It is widely used in several applications, such as, electrical systems, biological systems, etc [1]. The fractional behaviour helps to model a real object more accurately than the integer order model. For the past several years, the integer order models were used due to the absence of solution methods for fractional equations [2]. Numerous methods are used for approximation of fractional derivatives and integrals. Among them the fractional calculus can easily be used for wide area of applications.

Inductors and capacitors, the key components of power electronic converters, are usually considered as integer-order

components in the traditional models of power electronic converters. However, it cannot reflect their actual operating characteristics [3]. In recent years, the fractional-order modelling of power electronic converters are approached by considering the fractional-order characteristics of inductors and capacitors [4].

Researchers have accomplished considerable progress in the application of fractional order electrical circuits and components. Number of models related to fractional order inductors and capacitors are built [5]. The study on inductors and capacitors shows their fractional nature and can be modelled using fractional calculus to describe their electrical characteristics [6]. Fractional order components provide flexibility and freedom in circuit design [5]. Researchers have worked on the fractional behaviour of inductors and capacitors under different dielectrics [4], [7]. Fractional order capacitor is developed using different fractal structure [8]. The fractional order inductors of different orders can be developed based on skin effect [9]. The fractional behaviour indicates the possibility of being deployed in practical applications of power electronic converters.

Fractional modelling of power electronic systems i.e. dc-dc converter, is reported in literature [10]–[12]. The fractional-order modelling and analysis of a three-phase voltage source PWM rectifier (VSR) is presented recently considering the fractional-order characteristics of actual inductors and capacitors. While the Caputo fractional calculus operator is used to describe the fractional-order characteristics of an inductor and a capacitor, the fractional-order model of a three-phase VSR is established in the three-phase static coordinate system [3]. However, the stability analysis and detailed analytical study to establish the fractional theory for power electronic converters is missing. It needs to be carried out to establish the fractional-order modelling for power electronic converter applications. As reported, the frequency domain analysis proves that the order of model has significant influence on the stability performance of power electronic converters [13], [14].

In this paper, fractional order modelling of Voltage Source Converter (VSC) using fractional calculus is established and analysed in detail. Caputo derivative is considered as smooth fractional derivative and utilised to develop state-space model of fractional order VSC. The mathematical modelling of fractional order VSC is done considering fractional capacitor and inductor as the integral part of VSC system. Detailed investigation is carried out on developed mathematical fractional order model of VSC including small-signal and DC analysis. Time-domain modelling and extensive stability studies are presented with experimental verifications based on fractional order inductor and capacitors. Results are in comparison with the integer order VSC for performance evaluation of fractional order VSC. This study is also validated by real-time simulation experiments in order to verify VSC performance and analysis. The stability studies and time-domain transient analysis are carried out using real-time simulator to validate the fractional order VSC, for its real-time application as Distribution STATtic COMpensator (DSTATCOM) in power distribution system.

The layout of paper is as follow: Section II introduces background of fractional calculus. The fractional order modelling of VSC is provided in section III. Average state space analysis is discussed in section IV. Section V and section VI describes the dc analysis and small signal analysis of VSC. The performance of fractional order VSC is compared with integer order VSC in section VII. Time domain analysis on the fractional order system is reported in section VIII. In section IX, the work is concluded.

II. INTRODUCTION OF FRACTIONAL CALCULUS

Fractional calculus is a mathematical approach that deals with integrals and derivatives of arbitrary and complex orders. The operator ${}_aD_t^q$, depending upon the sign of q denotes that it is fractional integrator or fractional differentiator. The operator is defines as:

$$ {}_aD_t^q = \begin{cases} \dfrac{\partial^q}{\partial t^q} & \mathrm{q} > 0 \\ 1 & \mathrm{q} = 0 \\ \displaystyle\int_a^t (\partial\tau)^{-q} & \mathrm{q} < 0 \end{cases} \tag{1} $$

where q is a fractional operator and a, t are the operational limits [2]. Caputo derivative is considered as smooth fractional derivative and is defined as follows:

$$ {}_aD_t^q f(t) = \begin{cases} \dfrac{1}{\Gamma(n-q)} \displaystyle\int_a^t \frac{f^n(\tau)}{(t-q)^{q+1-n}} \partial\tau & \mathrm{n-1 < q < n} \\ \dfrac{\partial^n}{\partial t^n f(t)} & \mathrm{q} = n \end{cases} \tag{2} $$

where gamma (Γ) function is defined as

$$ \Gamma(x) = \int_0^\infty t^{x-1} e^{-1} \partial t \tag{3} $$

Taking laplace transform of (2). The equation can be written as

$$ L\{{}_aD_t^q f(t)\} = s^q F(s) - \sum_{k=0}^{n-1} s^{q-k-1} f^k(0) \quad \mathrm{n-1 < q < n} \tag{4} $$

where $n \in N$. Laplace transform of caputo derivative as stated by (2) while considering initial condition to be zero is given as:

$$ L\{{}_aD_t^q f(t)\} = s^q F(s) \tag{5} $$

The fractional order differential equation can be represented in the following form as stated by (6) [1].

$$ \begin{aligned} &a_n D^{q_n} y(t) + a_{n-1} D^{q_{n-1}} y(t) \ldots\ldots + a_0 D^{q_0} x(t) \\ &\quad = b_m D^{p_m} x(t) + b_{m-1} D^{p_{m-1}} x(t) \ldots\ldots + b_0 D^{p_0} x(t) \end{aligned} \tag{6} $$

D^{q_n} and D^{p_m} are caputo fractional derivative. $a_k (k = 0 \ldots n)$ and $b_k (k = 0 \ldots n)$ are constants and $q_k (k = 0..n)$,

$p_k(k = 0..n)$ are any arbitrary real and rational numbers. Laplace transform of (6) is given as

$$G(s) = \frac{Y(s)}{X(s)} = \frac{b_m D^{p_m} \ldots + b_1 D^{p_1} + b_0 D^{p_0}}{a_n D^{q_n} \ldots + a_1 D^{q_1} + a_0 D^{q_0}} \tag{7}$$

$Y(s)$ and $X(s)$ represent the laplace transform of output and input. In state-space model, fractional order linear time invariant system can also be represented by (8) [15].

$$\begin{aligned} \partial^p x(t) &= Ax(t) + Bu(t) \\ y(t) &= Cx(t) + Du(t) \end{aligned} \tag{8}$$

III. MATHEMATICAL MODELLING OF VOLTAGE SOURCE CONVERTER

The three-phase line diagram of Distribution STATic COMpensator (DSTATCOM) in power distribution system which consists of IGBTs based VSC and a dc capacitor C_{dc} is shown in Fig.1. The modelling of DSTATCOM is based on synchronous reference frame theory. The d and q axis are assumed to be rotating at a constant velocity "ω"rad/sec ($\omega = 2\pi f$) in an anticlockwise direction. Loading is considered as RL load.

The $a - b - c$ variables are converted into $d - q$ variables using park transformation [16]. During transformation three-phase quantities are transformed into stationary reference frame and further into rotating frame. Following assumptions are considered during transformation [17]:

- The zero sequence and sinusoidal components are absent.
- Semiconductor devices in converter are ideal.
- Losses due to shunt impedance and harmonics are negligible.
- Voltage source is considered as balanced source.

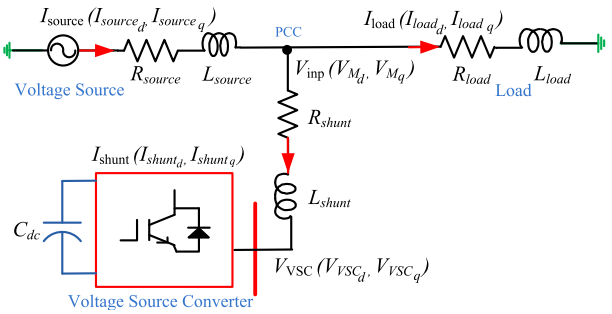

FIGURE 1. Line diagram of power distribution system with voltage source converter as DSTATCOM.

A. DIFFERENTIAL EQUATIONS AT SOURCE END

Applying KVL in Fig. 1 between voltage source and Point of Common Coupling (PCC). The equations can be written as:

$$\begin{aligned} \frac{\partial^\alpha I_{source_d}}{\partial t^\alpha} &= \frac{\omega * I_{source_q}}{L_{source}} - \frac{R_{source} I_{source_d}}{L_{source}} \\ &+ \frac{V_{source_d} - V_{M_d}}{L_{source}} \end{aligned} \tag{9}$$

$$\begin{aligned} \frac{\partial^\alpha I_{source_q}}{\partial t^\alpha} &= -\frac{\omega * I_{source_d}}{L_{source}} - \frac{R_{source} I_{source_q}}{L_{source}} \\ &+ \frac{V_{source_q} - V_{M_q}}{L_{source}} \end{aligned} \tag{10}$$

B. DIFFERENTIAL EQUATIONS AT LOAD END

Applying KVL at load end in Fig. 1. The equation can be written as:

$$\frac{\partial^\alpha I_{load_d}}{\partial t^\alpha} = \frac{\omega * I_{load_q}}{L_{load}} - \frac{R_{load} I_{load_d}}{L_{load}} + \frac{V_{M_d}}{L_{load}} \tag{11}$$

$$\frac{\partial^\alpha I_{load_q}}{\partial t^\alpha} = -\frac{\omega * I_{load_d}}{L_{load}} - \frac{R_{load} I_{load_q}}{L_{load}} + \frac{V_{M_q}}{L_{load}} \tag{12}$$

C. DIFFERENTIAL EQUATIONS AT SHUNT PART

Applying KVL in Fig. 1 between VSC and PCC. The equation at shunt end can be written as:

$$\frac{\partial^\alpha I_{shunt_d}}{\partial t^\alpha} = \frac{\omega * I_{shunt_q}}{L_{shunt}} - \frac{R_{shunt} I_{shunt_d}}{L_{shunt}} + \frac{V_{M_d} - V_{vsc_d}}{L_{shunt}} \tag{13}$$

$$\frac{\partial^\alpha I_{shunt_q}}{\partial t^\alpha} = -\frac{\omega * I_{shunt_d}}{L_{shunt}} - \frac{R_{shunt} I_{shunt_q}}{L_{shunt}} + \frac{V_{M_q} - V_{vsc_q}}{L_{shunt}} \tag{14}$$

D. STATE-SPACE REPRESENTATION OF VOLTAGE SOURCE CONVERTER

Using power balance equation on VSC and dc-side of VSC is given by (15)

$$P_{dc} = P_{vsc} \tag{15}$$

where P_{dc} is the power on dc side of VSC and P_{vsc} is the power on ac side of VSC. As $P_{dc} = V_{dc} * I_{dc}$ where value of $V_{dc} * I_{dc}$ is given by (16)

$$V_{dc} * I_{dc} = \frac{3}{2}(V_{vsc_d} I_{shunt_d} + V_{vsc_q} I_{shunt_q}) \tag{16}$$

Current across a capacitor can be written as:

$$I_{dc} = C_{dc} \frac{\partial^\beta V_{dc}}{\partial t^\beta} \tag{17}$$

From (16) and (17), dc link voltage of fractional order β is given as:

$$\frac{\partial^\beta V_{dc}}{\partial t^\beta} = \frac{3}{2C_{dc} V_{dc}}(V_{vsc_d} I_{shunt_d} + V_{vsc_q} I_{shunt_q}) \tag{18}$$

The shunt current for dq variables of fractional order α can be represented using (13) and (14) as:

$$\frac{\partial^\alpha I_{shunt_d}}{\partial t^\alpha} = \frac{1}{L_{shunt}}(V_{M_d} - V_{vsc_d} - R_{shunt} I_{shunt_d} + \omega I_{shunt_q}) \tag{19}$$

$$\frac{\partial^\alpha I_{shunt_q}}{\partial t^\alpha} = \frac{1}{L_{shunt}}(V_{M_q} - V_{vsc_q} - R_{shunt} I_{shunt_q} - \omega I_{shunt_d}) \tag{20}$$

The relation between capacitor voltage (V_{dc}), VSC volatge (V_{vsc}) and the duty ratio (d_{abc}) is given by:

$$\begin{bmatrix} d_a \\ d_b \\ d_c \end{bmatrix} = \begin{bmatrix} 1/2 \\ 1/2 \\ 1/2 \end{bmatrix} + \frac{1}{V_{dc}} \begin{bmatrix} V_{vsc_a} \\ V_{vsc_b} \\ V_{vsc_c} \end{bmatrix} \tag{21}$$

By using Park's transformation in (21), *abc* to *dq*0 transformation is done and given by:

$$d_d = \frac{V_{vsc_d}}{V_{dc}} \tag{22}$$

$$d_q = \frac{V_{vsc_q}}{V_{dc}} \tag{23}$$

$$d_0 = \frac{1}{2} + \frac{V_{vsc_d}}{V_{dc}} \tag{24}$$

In general, state-space model can be written as similar to (8),

$$\begin{aligned} \dot{X} &= [A]X + [B]U \\ Y &= [C]X \end{aligned} \tag{25}$$

By using (18), (19), (20) and representing in state-space model form is given below:

$$\begin{bmatrix} \frac{\partial^\alpha I_{shunt_d}}{\partial t^\alpha} \\ \frac{\partial^\alpha I_{shunt_q}}{\partial t^\alpha} \\ \frac{\partial^\beta V_{dc}}{\partial t^\beta} \end{bmatrix} = \begin{bmatrix} -\frac{R_{shunt}}{L_{shunt}} & \omega & -\frac{d_d}{L_{shunt}} \\ -\omega & -\frac{R_{shunt}}{L_{shunt}} & -\frac{d_q}{L_{shunt}} \\ \frac{3}{2C_{dc}}(d_d) & \frac{3}{2C_{dc}}(d_q) & 0 \end{bmatrix} \begin{bmatrix} I_{shunt_d} \\ I_{shunt_q} \\ V_{dc} \end{bmatrix} + \begin{bmatrix} \frac{1}{L_{shunt}} & 0 \\ 0 & \frac{1}{L_{shunt}} \\ 0 & 0 \end{bmatrix} \begin{bmatrix} V_{M_d} \\ V_{M_q} \\ 0 \end{bmatrix} \tag{26}$$

$$V_0 = \begin{bmatrix} 0 & 0 & 1 \end{bmatrix} \begin{bmatrix} I_{shunt_d} \\ I_{shunt_q} \\ V_{dc} \end{bmatrix} \tag{27}$$

In (26) and (27), fractional state-space model is obtained for VSC, where the additional parameters α and β represent the fractional order of inductor (L_{shunt}) and capacitor (C_{dc}), respectively. Thus, from (26) and (27), state-space model parameters **A**, **B** and **C** can be represented as follow:

$$A = \begin{bmatrix} -\frac{R_{shunt}}{L_{shunt}} & \omega & -\frac{d_d}{L_{shunt}} \\ -\omega & -\frac{R_{shunt}}{L_{shunt}} & -\frac{d_q}{L_{shunt}} \\ \frac{3}{2C_{dc}}(d_d) & \frac{3}{2C_{dc}}(d_q) & 0 \end{bmatrix};$$

$$B = \begin{bmatrix} \frac{1}{L_{shunt}} & 0 \\ 0 & \frac{1}{L_{shunt}} \\ 0 & 0 \end{bmatrix};$$

$$C = \begin{bmatrix} 0 & 0 & 1 \end{bmatrix} \tag{28}$$

where **A** is a state matrix, **B** is input matrix and **C** is output matrix.

IV. AVERAGE STATE-SPACE MODEL OF FRACTIONAL ORDER VSC

In this section, average state-space model of fractional order VSC is developed by dividing state-space equation into ac and dc parts. Averaging is done over a period of switching to eliminate higher order switching harmonics. Average formula thus obtained is further used for dc and and small-signal analysis of fractional order VSC.

Averaging formula states that

$$< x(t) >_T = \frac{1}{T} \int_t^{t+T} x(\tau) \partial \tau \tag{29}$$

where x is any arbitrary variable of VSC [18].

$$\frac{\partial < x(t) >_T^\alpha}{\partial t^\alpha} = \langle \frac{\partial^\alpha x(t)}{\partial t^\alpha} \rangle_T \tag{30}$$

The variables in VSC consists of dc and ac components where i_{shunt_d} and $\hat{i}_{shunt_d}(t)$ are dc and ac terms. Various terms can be represented in dc and ac terms as follows:

$$\begin{aligned} \langle I_{shunt_d}(t) \rangle &= i_{shunt_d} + \hat{i}_{shunt_d}(t), \\ \langle I_{shunt_q}(t) \rangle &= i_{shunt_q} + \hat{i}_{shunt_q}(t), \\ \langle V_{dc} \rangle &= v_{dc} + \hat{v}_{dc}(t), \\ \langle c(t) \rangle &= D + \hat{c}(t), \\ \langle V_{inp}(t) \rangle &= v_{inp} + \hat{v}_{inp}(t), \end{aligned} \tag{31}$$

where $V_{inp}(t) = \begin{bmatrix} V_{M_d} \\ V_{M_q} \\ 0 \end{bmatrix}$

Let $c(t)$ be the switched on state of VSC, $c(t) = \frac{T_{on}}{T}$ and D is the duty cycle. For an ideal switch, the switching function is expressed as

$$c(t) = \begin{cases} 1 & \text{c on;} \\ 0 & \text{c off;} \end{cases} \tag{32}$$

The dead zone case is excluded in this theoretical work [19]. Average state-space model of (25) and (26) can be written as (33):

$$\begin{bmatrix} \frac{\partial^\alpha \langle I_{shunt_d} \rangle}{\partial t^\alpha} \\ \frac{\partial^\alpha \langle I_{shunt_q} \rangle}{\partial t^\alpha} \\ \frac{\partial^\beta \langle V_{dc} \rangle}{\partial t^\beta} \end{bmatrix} = \begin{bmatrix} -\frac{R_{shunt}}{L_{shunt}} & \omega & -\frac{d_d}{L_{shunt}} \\ -\omega & -\frac{R_{shunt}}{L_{shunt}} & -\frac{d_q}{L_{shunt}} \\ \frac{3}{2C_{dc}}(d_d) & \frac{3}{2C_{dc}}(d_q) & 0 \end{bmatrix} \begin{bmatrix} \langle I_{shunt_d} \rangle \\ \langle I_{shunt_q} \rangle \\ \langle V_{dc} \rangle \end{bmatrix} + \begin{bmatrix} \frac{\langle c(t) \rangle}{L_{shunt}} & 0 \\ 0 & \frac{\langle c(t) \rangle}{L_{shunt}} \\ 0 & 0 \end{bmatrix} \begin{bmatrix} \langle V_{inp} \rangle \end{bmatrix} \tag{33}$$

The average value of used variable is replaced by their dc and ac components as given in (34).

$$\begin{bmatrix} \frac{\partial^\alpha (i_{shunt_d} + \hat{i}_{shunt_d}(t))}{\partial t^\alpha} \\ \frac{\partial^\alpha (i_{shunt_q} + \hat{i}_{shunt_q}(t))}{\partial t^\alpha} \\ \frac{\partial^\beta (v_{dc} + \hat{v}_{dc}(t))}{\partial t^\beta} \end{bmatrix}$$

$$= \begin{bmatrix} -\frac{R_{shunt}}{L_{shunt}} & \omega & -\frac{d_d}{L_{shunt}} \\ -\omega & -\frac{R_{shunt}}{L_{shunt}} & -\frac{d_q}{L_{shunt}} \\ \frac{3}{2C_{dc}}(d_d) & \frac{3}{2C_{dc}}(d_q) & 0 \end{bmatrix} \times \begin{bmatrix} (i_{shunt_d} + \hat{i}_{shunt_d}(t)) \\ (i_{shunt_q} + \hat{i}_{shunt_q}(t)) \\ (v_{dc} + \hat{v}_{dc}(t)) \end{bmatrix} + \begin{bmatrix} \frac{D + c(\hat{t})}{L_{shunt}} & 0 \\ 0 & \frac{D + c(\hat{t})}{L_{shunt}} \\ 0 & 0 \end{bmatrix} \left[v_{inp} + \hat{v}_{inp}(t) \right] \quad (34)$$

V. DC ANALYSIS OF VSC

DC analysis is done to determine the branch current and dc-link voltage of the VSC. The ac values are omitted in case of dc analysis and the averaged values obtained in (34) are substituted in (25). Caputo derivative is zero for dc components and the following equation can be achieved as stated in (35).

$$0 = [A] \begin{bmatrix} i_{shunt_d} \\ i_{shunt_q} \\ v_{dc} \end{bmatrix} + [B]U \quad (35)$$

$$\begin{bmatrix} i_{shunt_d} \\ i_{shunt_q} \\ v_{dc} \end{bmatrix} = -[A]^{-1}[B]U \quad (36)$$

$$\begin{bmatrix} i_{shunt_d} \\ i_{shunt_q} \\ v_{dc} \end{bmatrix} = -\frac{1}{\Delta} \times \begin{bmatrix} \frac{Dd_q^2}{2C_{dc}L_{shunt}^2} & -\frac{D^3 d_q d_d}{2C_{dc}L_{shunt}^2} \\ -\frac{3d_q d_d D}{2C_{dc}L_{shunt}^2} & \frac{3d_d^2 D}{2C_{dc}L_{shunt}^2} \\ D\frac{R_{shunt}d_d}{L_{shunt}^3} + \frac{\omega d_q}{L_{shunt}^2} & -\frac{d_q R_{shunt} D}{L_{shunt}^3} + \frac{d_d \omega D}{L_{shunt}^2} \end{bmatrix} \quad (37)$$

where $\Delta = \frac{-R_{shunt}d_q^2}{2L_{shunt}C_{dc}L_{shunt}} - \frac{3\omega d_q d_d}{2\,C_{dc}L_{shunt}} + \frac{3\omega d_d d_q}{L_{shunt}C_{dc}} - \frac{3\,d_d^2 R_{shunt}}{2L_{shunt}^2 C_{dc}}$

Equation (37) gives the shunt current for dq variables and dc-link voltage provided to VSC.

VI. SMALL SIGNAL ANALYSIS OF VSC

Large signal analysis allows to find DC operating point of the system whereas small signal analysis helps to find the result of applying a small signal on top of the DC operating points of the system. In small signal analysis, dc components are neglected and considering only ac part of (34) is given as

$$\begin{bmatrix} \frac{\partial^\alpha \hat{i}_{shunt_d}(t)}{\partial t^\alpha} \\ \frac{\partial^\alpha \hat{i}_{shunt_q}(t)}{\partial t^\alpha} \\ \frac{\partial^\beta \hat{v}_{dc}(t)}{\partial t^\beta} \end{bmatrix} = \begin{bmatrix} -\frac{R_{shunt}}{L_{shunt}} & \omega & -\frac{d_d}{L_{shunt}} \\ -\omega & -\frac{R_{shunt}}{L_{shunt}} & -\frac{d_q}{L_{shunt}} \\ \frac{3}{2C_{dc}}(d_d) & \frac{3}{2C_{dc}}(d_q) & 0 \end{bmatrix} \begin{bmatrix} \hat{i}_{shunt_d}(t) \\ \hat{i}_{shunt_q}(t) \\ \hat{v}_{dc}(t) \end{bmatrix} + \begin{bmatrix} \frac{D}{L_{shunt}} & 0 \\ 0 & \frac{D}{L_{shunt}} \\ 0 & 0 \end{bmatrix} \begin{bmatrix} \hat{v}_{inp}(t) \end{bmatrix} + \begin{bmatrix} \frac{v_{inp}}{L_{shunt}} & 0 \\ 0 & \frac{v_{inp}}{L_{shunt}} \\ 0 & 0 \end{bmatrix} \begin{bmatrix} \hat{c}(t) \end{bmatrix} \quad (38)$$

From (38), averaged small-signal analysis of VSC can be rewritten as (39)-(41).

$$\frac{\partial^\alpha (\hat{i}_{shunt_d}(t))}{\partial t^\alpha} = -\frac{R_{shunt}}{L_{shunt}}\hat{i}_{shunt_d}(t) + \omega \hat{i}_{shunt_q}(t) - \frac{d_d}{L_{shunt}}\hat{v}_{dc}(t) + \frac{D}{L_{shunt}}\hat{v}_{inp}(t) + \frac{v_{inp}}{L_{shunt}}\hat{c}(t) \quad (39)$$

$$\frac{\partial^\alpha \hat{i}_{shunt_q}(t)}{\partial t^\alpha} = -\omega \hat{i}_{shunt_d}(t) - \frac{R_{shunt}}{L_{shunt}}\hat{i}_{shunt_q}(t) - \frac{d_q}{L_{shunt}}\hat{v}_{dc}(t) + \frac{D}{L_{shunt}}\hat{v}_{inp}(t) + \frac{v_{inp}}{L_{shunt}}\hat{c}(t) \quad (40)$$

$$\frac{\partial^\beta \hat{v}_{dc}(t)}{\partial t^\beta} = \frac{3}{2C_{dc}}(d_d)\hat{i}_{shunt_d}(t) + \frac{3}{2C_{dc}}(d_q)\hat{i}_{shunt_q}(t) \quad (41)$$

Taking Laplace transform of (39)-(41), while considering zero initial condition is stated below:

$$s^\alpha \hat{i}_{shunt_d}(s) = -\frac{R_{shunt}}{L_{shunt}}\hat{i}_{shunt_d}(s) + \omega \hat{i}_{shunt_q}(s) - \frac{d_d}{L_{shunt}}\hat{v}_{dc}(s) + \frac{D}{L_{shunt}}\hat{v}_{inp}(s) + \frac{v_{inp}}{L_{shunt}}\hat{c}(s) \quad (42)$$

$$s^\alpha \hat{i}_{shuntq}(s) = -\omega \hat{i}_{shunt_d}(s) - \frac{R_{shunt}}{L_{shunt}}\hat{i}_{shunt_q}(s) - \frac{d_q}{L_{shunt}}\hat{v}_{dc}(s) + \frac{D}{L_{shunt}}\hat{v}_{inp}(s) + \frac{v_{inp}}{L_{shunt}}\hat{c}(s) \quad (43)$$

$$s^\beta \hat{v}_{dc}(s) = \frac{3}{2C_{dc}}(d_d)\hat{i}_{shunt_d}(s) + \frac{3}{2C_{dc}}(d_q)\hat{i}_{shunt_q}(s) \quad (44)$$

Equation (44) can be rewritten as

$$\hat{i}_{shunt_d}(s) = \frac{2C_{dc}}{3d_d}s^\beta \hat{v}_{dc}(s) - \frac{d_q}{d_d}\hat{i}_{shunt_q}(s) \quad (45)$$

$$\hat{i}_{shunt_q}(s) = \frac{2C_{dc}}{3d_q}s^\beta \hat{v}_{dc}(s) - \frac{d_d}{d_q}\hat{i}_{shunt_d}(s) \quad (46)$$

By substituting (45) in (42) and re-writing as given below:

$$s^\alpha\left(\frac{2C_{dc}}{3d_d}s^\beta \hat{v}_{dc}(s) - \frac{d_q}{d_d}\hat{i}_{shunt_q}(s)\right) = -\frac{R_{shunt}}{L_{shunt}}\left(\frac{2C_{dc}}{3d_d}s^\beta \hat{v}_{dc}(s) - \frac{d_q}{d_d}\hat{i}_{shunt_q}(s)\right)$$

$$+\omega\hat{i}_{shunt_q}(s)-\frac{d_d}{L_{shunt}}\hat{v}_{dc}(s)+\frac{D}{L_{shunt}}\hat{v}_{inp}(s)+\frac{v_{inp}}{L_{shunt}}\hat{c}(s) \quad (47)$$

Assuming q component to be zero. Above equation can be rewritten as

$$s^{\alpha+\beta}\frac{2C_{dc}}{3d_d}\hat{v}_{dc}(s)=-\frac{R_{shunt}}{L_{shunt}}\frac{2C_{dc}}{3d_d}s^{\beta}\hat{v}_{dc}(s)-\frac{d_d}{L_{shunt}}\hat{v}_{dc}(s)+\frac{D}{L_{shunt}}\hat{v}_{inp}(s)+\frac{v_{inp}}{L_{shunt}}\hat{c}(s) \quad (48)$$

The transfer function of dc-link voltage and bus voltage at PCC is given by (49).

$$G_{\hat{v}_{dc}-\hat{v}_{inp}}=\frac{\hat{v}_{dc}}{\hat{v}_{inp}}|_{\hat{c}(s)=0}=\frac{D}{(s^{\alpha+\beta}\frac{2C_{dc}}{3d_d}L_{shunt}+\frac{s^{\beta}2C_{dc}R_{shunt}}{d_d}+d_d)} \quad (49)$$

In order to obtain transfer function for q variable, on substituting (46) in (43) and re-writing as given below:

$$s^{\alpha}(\frac{2C_{dc}}{3d_q}s^{\beta}\hat{v}_{dc}(s)-\frac{d_d}{d_q}\hat{i}_{shunt_d}(s))=-\omega\hat{i}_{shunt_d}(s)-\frac{R_{shunt}}{L_{shunt}}(\frac{2C_{dc}}{3d_q}s^{\beta}\hat{v}_{dc}(s)-\frac{d_d}{d_q}\hat{i}_{shunt_d}(s))-\frac{d_q}{L_{shunt}}\hat{v}_{dc}(s)+\frac{D}{L_{shunt}}\hat{v}_{inp}(s)+\frac{v_{inp}}{L_{shunt}}\hat{d}(s) \quad (50)$$

$$G_{\hat{v}_{dc}-\hat{v}_{inp}}=\frac{\hat{v}_{dc}}{\hat{v}_{inp}}|_{\hat{c}(s)=0}=\frac{D}{(s^{\alpha+\beta}\frac{2C_{dc}}{3d_q}L_{shunt}+\frac{s^{\beta}2C_{dc}R_{shunt}}{3d_q}+d_q)} \quad (51)$$

The relation between dc output voltage across VSC and input voltage applied across VSC is given by (49) and (51), respectively. The relationship between duty cycle and output voltage is obtained by substituting (45) in (42) while ignoring input voltage and as given in (52):

$$s^{\alpha}(\frac{2C_{dc}}{3d_d}s^{\beta}\hat{v}_{dc}(s)-\frac{d_q}{d_d}\hat{i}_{shunt_q}(s))=-\frac{R_{shunt}}{L_{shunt}}(\frac{2C_{dc}}{3d_d}s^{\beta}\hat{v}_{dc}(s)-\frac{d_q}{d_d}\hat{i}_{shunt_q}(s))+\omega\hat{i}_{shunt_q}(s)-\frac{d_d}{L_{shunt}}\hat{v}_{dc}(s)+\frac{D}{L_{shunt}}\hat{v}_{inp}(s)+\frac{v_{inp}}{L_{shunt}}\hat{c}(s) \quad (52)$$

Neglecting q component and considering input voltage equals to zero in (52) gives:

$$s^{\alpha+\beta}\frac{2C_{dc}}{3d_d}\hat{v}_{dc}(s)+\frac{R_{shunt}}{L_{shunt}}\frac{2C_{dc}}{3d_d}s^{\beta}\hat{v}_{dc}(s)+\frac{d_d}{L_{shunt}}\hat{v}_{dc}(s)=\frac{v_{inp}}{L_{shunt}}\hat{c}(s) \quad (53)$$

$$G_{\hat{v}_{dc}-\hat{c}(s)}=\frac{\hat{v}_{dc}}{\hat{d}(s)}|_{\hat{v}_{inp}(s)=0}=\frac{v_{inp}}{(s^{\alpha+\beta}\frac{2C_{dc}}{3d_d}L_{shunt}+\frac{s^{\beta}2C_{dc}R_{shunt}}{d_d}+d_d)} \quad (54)$$

The transfer function given in (54) shows the ratio of output dc-link voltage and duty cycle while considering input voltage equal to zero.

VII. PERFORMANCE EVALUATION OF FRACTIONAL ORDER VSC

This section presents the performance analysis of Fractional order model in comparison to integer order model. Table 1 shows the parameter used during analysis of VSC. The integer order inductors and capacitors used for VSC modelling are assumed to be accurate enough for the existing system. The transfer function for integer order model is obtained from (49) while considering parameters of Table 1 and given by (55).

$$G_{\hat{v}_{dc}-\hat{v}_{inp}}=\frac{0.0008}{4.489e-07s^2+0.0002687s+6.4e-05} \quad (55)$$

where fractional order of inductor (α) and capacitor (β) are assumed to be an integer value of order one. The control gain of VSC is stable for 0.1 to 0.9 duty cycle range [20]. The averaged value of duty cycle is considered as 0.5 in (55) and (56). Different fractional order values of α and β are considered for the analysis of fractional order VSC.

The fractional order transfer function of VSC as stated in (49) for α and $\beta = 1.2$ is given as

$$G_{\hat{v}_{dc}-\hat{v}_{inp}}=\frac{0.0008}{4.489e-07s^{2.4}+0.0002687s^{1.2}+6.4e-05} \quad (56)$$

To analyse the stability of system at different values of (α, β), comparison between the bode plots of fractional and integer order system is done and presented in Fig. 2. The simulation has been carried out using Matlab where FOMCON library is used to perform fractional calculus. Gain margin and phase margin in bode plot signifies about the stability of system. For integer order transfer function case (where (α, β) = 1), the gain margin is 4.0525^{+07} and phase margin is 94.3045°. The gain margin and phase margin of integer order transfer function is compared with different fractional order transfer functions to analyse the system. Greater the gain margin and phase margin greater will be the stability of the system. The gain margin starts deteriorating when values of (α, β) is considered more than one.

The comparison between step response for integer and fractional order system as given by (55) and (56) is shown in Fig. 2. The purpose of considering the fractional order more than one is to check the impact on the stability of system. The step response in Fig. 2 for (α, β) = (1.2, 1.2) and (1.6, 1.6) shows that integer order model for (α, β) = (1, 1) is more stable in comparison to fractional order model. Different values of fractional order is considered in (49) where (α, β) = 0.9, 0.8 and 0.5 to evaluate the performance of fractional order VSC on stability factor. Fig. 3 shows the performance at different fractional orders of VSC. Table 2 shows the gain margin and phase margin obtained for different values of α and β.

In fractional order model, the gain margin of the system increases as value of (α, β) < 1. In case of (α, β) = 0.8 and

TABLE 1. System parameters.

Parameters	Symbol	Value
RMS Voltage(L-L)	V_{source}	220V
Fundamental Frequency	f	50Hz
Angular Frequency	ω	314rsd/sec
dc Link Capacitor	C_{dc}	6500μF
Transmission Line	R_{source} L_{source}	0.27Ω 8.2mH
Shunt Transformer	R_{shunt} L_{shunt}	1.55 Ω 3mH
Load Parameters	R_{load} L_{load}	13.6 Ω 10.2mH
DC Reference	DC_{ref}	600V
Resistive Linear Load	R_l	100Ω
RL Load 1	R_{load1} L_{load1}	50 Ω 5mH
RL Load 2	R_{load2} L_{load2}	100 Ω 0.0005mH

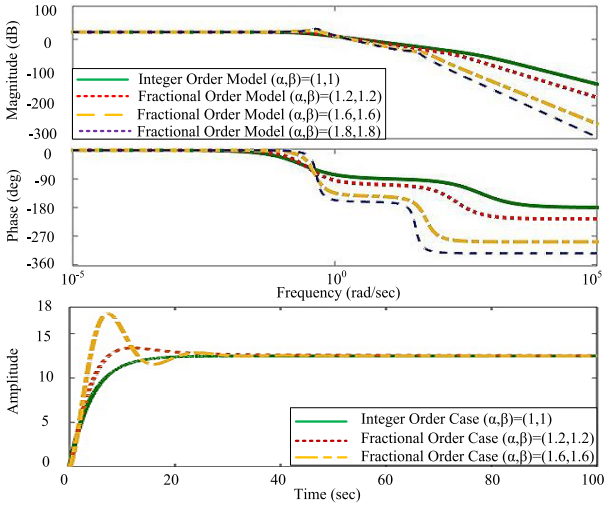

FIGURE 2. Frequency response and step response of transfer function for integer order model and fractional order model.

0.5 the gain margin will become very large and the system will remain stable for a very high range of frequencies.

Dc value of input voltage is considered 50V and the fractional order transfer function of (54) at $(\alpha, \beta) = (0.8,0.8)$ can be written as (57).

$$G_{\hat{v}_{dc}-\hat{d}(s)} = \frac{50}{4.489e-07s^{1.6} + 0.0002687s^{0.8} + 6.4e-05} \tag{57}$$

The random value of (α, β) are considered for simulation and comparison case between 0.1 to 2. The transfer function of (49) for fractional order case of VSC with $(\alpha = \beta = 0.8)$ is provided in (58). The step response is plotted which have same duty cycle and input voltage. The step response in Fig. 4 shows that in fractional order system becomes more stable but settling time increases as compare to integer order model as stated by (55).

$$G_{\hat{v}_{dc}-\hat{v}_{inp}} = \frac{0.0008}{4.489e-07s^{1.6}+0.0002687s^{0.8}+6.4e-05} \tag{58}$$

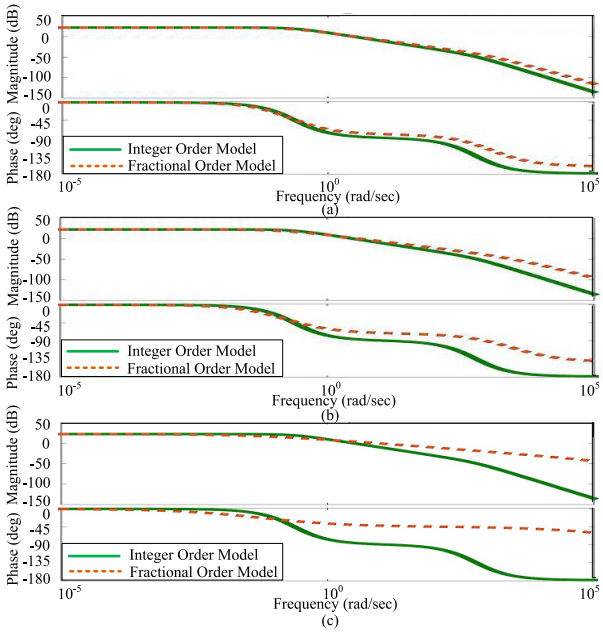

FIGURE 3. Frequency response of transfer function for integer order model at $(\alpha, \beta) = (1,1)$ and fractional order model at (a) $(\alpha, \beta) = (0.9,0.9)$, (b) $(\alpha, \beta) = (0.8,0.8)$, (c) $(\alpha, \beta) = (0.5,0.5)$.

TABLE 2. Frequency response at different fractional order.

Fractional Order	Gain margin	Phase margin
(α, β)=2	1.9016	0°
(α, β)=1.9	51.4399	9.6847°
(α, β)=1.8	55.4791	19.3139°
(α, β)=1.7	63.2275	28.9318°
(α, β)=1.6	76.7084	38.5040°
(α, β)=1.5	100.4432	48.0169°
(α, β)=1.4	145.4088	57.4573°
(α, β)=1.3	243.7960	66.8142°
(α, β)=1.2	526.1218	76.0788°
(α, β)=1.1	2.0534^{+03}	85.2436°
(α, β)=1	4.0525^{+07}	94.3045°
(α, β)=0.9	1.3384^{+21}	103.2587°
(α, β)=0.8	Very large	112.107°
(α, β)=0.5	Very large	138.0649°

VIII. TIME DOMAIN ANALYSIS

The layout of three-phase power distribution system is shown in Fig. 5. A full-wave rectifier supplying *RL* load is considered as non-linear load and used for the analysis of fractional order system. Initially pure resistive linear load of value of 100Ω is connected. But at 0.15 sec and 0.22 sec a non-linear load i.e. full-wave rectifier has been added with (50Ω, $5mH$) and (100Ω, $0.00005mH$), respectively at dc side of rectifier. The detailed parameters of complete system is given in Table-1.

A real-time simulator OP4510 $(OPAL - RT)^{TM}$ is used for simulation. In real-time simulator two subsystem are made known as master subsystem where hysteresis current controller is used for controlling voltage source inverter and console subsystem. In master subsystem the main controller is kept and in console the simulation results are seen.

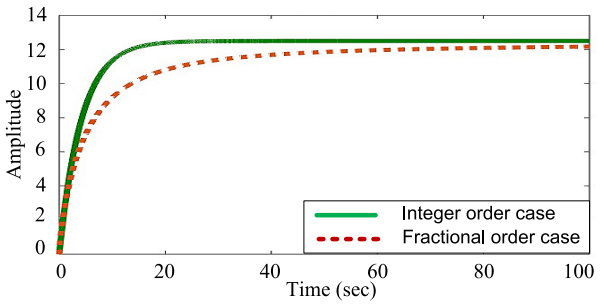

FIGURE 4. Step response for integer order model at (α, β) = (1,1) and fractional order model at (α, β) = (0.8,0.8).

The performance of system using fractional and integer order inductor and capacitor are verified using ac source currents and DC-link voltage.

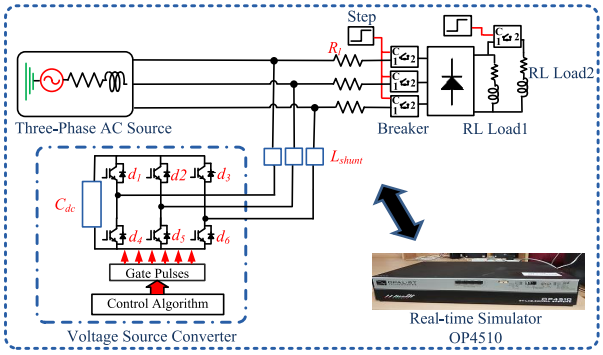

FIGURE 5. Layout of power distribution system using real time simulator.

A. IMPLEMENTATION OF FRACTIONAL-ORDER DEVICES

To develop simulation model of fractional order VSC with fractional order inductor and capacitor the chain fractance method is used as the fractional order inductor and capacitor are not present in simulation library. Similarly the real-time experimental fractional order inductor and capacitor can be physically realised using the chain fractance method due to un-availability in the market until now [10].

Mathematically, the impedance of any α-order inductor is defined as [10]:

$$Z_\alpha = (\jmath\omega)^\alpha = (\omega)^\alpha L[cos(\frac{\alpha\Pi}{2}) + \jmath sin(\frac{\alpha\Pi}{2})] \quad (59)$$

where the magnitude of Z_α should have a constant slope of 20 α db/dec and phases of $\frac{\alpha\Pi}{2}$. Similarly, for capacitor of order β, the impedance is defined as:

$$Z_\beta = \frac{1}{(\jmath\omega)^\beta} = \frac{1}{(\omega)^\beta C}[cos(\frac{\alpha\Pi}{2}) + \jmath sin(\frac{\alpha\Pi}{2})] \quad (60)$$

where the magnitude of Z_β should have a constant slope of -20 α db/dec and phases of $\frac{-\beta\Pi}{2}$.

From the frequency domain analysis, the value of α and β in the range $(0.5 \leq (\alpha = \beta) \leq 0.8)$ is considered to be more stable. In time domain analysis, the behaviour of

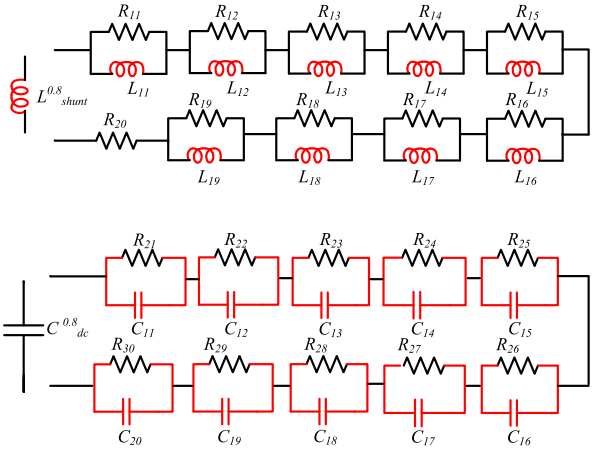

FIGURE 6. Fractional order inductor and capacitor in approximated model. Here $R_{11} = 7.16\,k\Omega$, $R_{12} = 340.84\Omega$, $R_{13} = 34.25\Omega$, $R_{14} = 3.54\,k\Omega$, $R_{15} = 367\,m\Omega$, $R_{16} = 38\,m\Omega$, $R_{17} = 4\,m\Omega$, $R_{18} = 0.4\,m\Omega$, $R_{19} = 42\,m\Omega$, $R_{20} = 5\mu\Omega$, $R_{21} = 20\,m\Omega$, $R_{22} = 160\,m\Omega$, $R_{23} = 1.5\Omega$, $R_{24} = 14.6\Omega$, $R_{25} = 141\,\Omega$, $R_{26} = 1.36\,k\Omega$, $R_{27} = 13.131\,m\Omega$, $R_{28} = 126.742\,k\Omega$, $R_{29} = 1.222\,M\Omega$, $R_{30} = 102.85\,M\Omega$, $L_{11} = 95\mu H$, $L_{12} = 77\mu H$, $L_{13} = 131.6\mu H$, $L_{14} = 231.6\mu H$, $L_{15} = 408\mu H$, $L_{16} = 719.4\mu H$, $L_{17} = 1.268\,mH$, $L_{18} = 2.235\,mH$, $L_{19} = 3.934\,mH$, $C_{11} = 6.5\mu F$, $C_{12} = 13.98\mu F$, $C_{13} = 24.5\mu F$, $C_{14} = 43.2\mu F$, $C_{15} = 76.2\mu F$, $C_{16} = 134.2\mu F$, $C_{17} = 236.6\mu F$, $C_{18} = 417\mu F$, $C_{19} = 736\mu F$, $C_{20} = 560\mu F$.

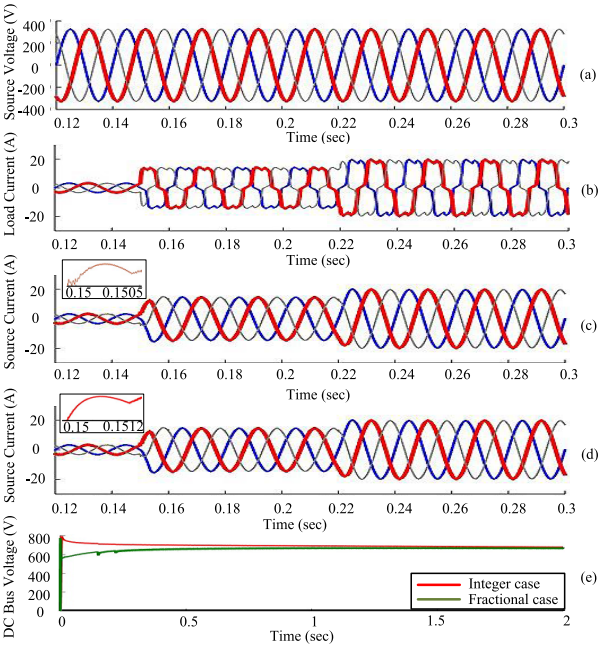

FIGURE 7. Performance evaluation of integer and fractional order model using real-time simulator for (a) Source voltage, (b) Load current, (c) Source current for integer order model, (d) Source current for fractional order model, (e) DC-link voltage.

fractional order inductor and capacitor is studied for ($\alpha = \beta = 0.8$) system. The approximate model of the fractional order inductor ($L_{shunt} = 3mH$ and $\alpha = 0.8$) and fractional order capacitor ($C_{bus} = 2500\mu F$ and $\beta = 0.8$) is shown in Fig. 6.

The rms voltage of 220V is provided and alignment based on synchronous reference frame theory is used for the

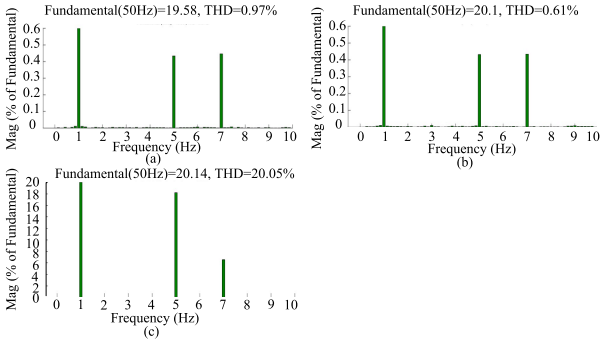

FIGURE 8. Total harmonic distortion of (a) Integer order model source current, (b) Fractional order model source current, (c) Non-linear load current.

generation of gate pulses [21]. The reference dc voltage of 600V is set. Fig. 7 shows the performance of VSC as DSTATCOM in power distribution system using fractional and integer order based inductors and capacitors. The dynamic response time under which source currents became sinusoidal after injection of non-linear load in system at time-instant of 0.15 sec is 0.5 msec using integer order inductors and capacitors as shown in Fig. 7(c). Fig. 7(d) shows the dynamic response using fractional order case is 1.2 msec. Fig. 7(e) represent the dc-link voltage of fractional and integer order models where the overshoot time of integer model is higher in comparison to fractional order model. The transient response is smooth in fractional order case and settling time is almost similar for both models. Total Harmonic Distortion (THD) reduction of source current for integer order model is from 20.05% to 0.97% and in fractional order model is from 20.05% to 0.61% as shown in Fig. 8.

IX. CONCLUSIONS

This paper proposes and presents a detailed mathematical modelling of Voltage Source Converter (VSC) using fractional calculus and caputo derivative method. Caputo derivative method eliminates complex definitions of fractional calculus. Approximate solution with optimal design of parameters can be obtained easily. Small-signal analysis and average state-space model based analysis has been developed for VSC. Performance analysis in terms of system stability has been carried out for fractional order model with different values of fractional order of inductor and capacitor i.e. α and β, respectively, and are compared with the integer order model. For the fractional-order VSC, state variables were dependent on model orders. Therefore, the change of fractional orders affects the stability and steady-state characteristics of the VSC. It is inferred from the simulation results, that when the orders of fractional devices reduces, the stability improves; however settling time increases. These phenomena have been explained by the mathematical analysis of the proposed modelling approach, and confirmed by extensive simulations results. Furthermore, the time-domain analysis has been done using real-time simulator for VSC for its application as DSTATCOM in power distribution system. The fractional order inductor and capacitor are implemented by using chain fractance method. The comparative results demonstrate superior transient response in case of fractional order devices as compared to integer order.

REFERENCES

[1] J. Sabatier, O. P. Agrawal, and J. T. Machado, *Advances in Fractional Calculus*, vol. 4, no. 9. Dordrecht, The Netherlands: Springer, 2007.
[2] I. Petráš, *Fractional-Order Nonlinear Systems: Modeling, Analysis and Simulation*. Springer, 2011.
[3] J. Xu, X. Li, H. Liu, and X. Meng, "Fractional-order modeling and analysis of a three-phase voltage source PWM rectifier," *IEEE Access*, vol. 8, pp. 13507–13515, 2020.
[4] A. Kartci, A. Agambayev, N. Herencsar, and K. N. Salama, "Series-, parallel-, and inter-connection of solid-state arbitrary fractional-order capacitors: Theoretical study and experimental verification," *IEEE Access*, vol. 6, pp. 10933–10943, 2018.
[5] M. S. Sarafraz and M. S. Tavazoei, "Passive realization of fractional-order impedances by a fractional element and RLC components: Conditions and procedure," *IEEE Trans. Circuits Syst. I, Reg. Papers*, vol. 64, no. 3, pp. 585–595, Mar. 2017.
[6] A. K. Jonscher, "Dielectric relaxation in solids," *J. Phys. D, Appl. Phys.*, vol. 32, no. 14, p. R57, 1999.
[7] S. Westerlund and L. Ekstam, "Capacitor theory," *IEEE Trans. Dielectr. Electr. Insul.*, vol. 1, no. 5, pp. 826–839, Oct. 1994.
[8] I. S. Jesus and J. A. T. Machado, "Development of fractional order capacitors based on electrolyte processes," *Nonlinear Dyn.*, vol. 56, nos. 1–2, pp. 45–55, Apr. 2009.
[9] J. A. T. Machado and A. M. S. F. Galhano, "Fractional order inductive phenomena based on the skin effect," *Nonlinear Dyn.*, vol. 68, nos. 1–2, pp. 107–115, Apr. 2012.
[10] X. Chen, Y. Chen, B. Zhang, and D. Qiu, "A modeling and analysis method for fractional-order DC–DC converters," *IEEE Trans. Power Electron.*, vol. 32, no. 9, pp. 7034–7044, Sep. 2017.
[11] A. G. Radwan, A. A. Emira, A. M. Abdelaty, and A. T. Azar, "Modeling and analysis of fractional order DC–DC converter," *ISA Trans.*, vol. 82, pp. 184–199, Nov. 2018.
[12] Y. Chen and B. Zhang, "Extension of ESPM to fractional-order DC/DC converters," in *Equivalent-Small-Parameter Analysis of DC/DC Switched-Mode Converter*. Singapore: Springer, 2019.
[13] S. Kamal, A. Raman, and B. Bandyopadhyay, "Finite-time stabilization of fractional order uncertain chain of integrator: An integral sliding mode approach," *IEEE Trans. Autom. Control*, vol. 58, no. 6, pp. 1597–1602, Jun. 2013.
[14] N. Yang, C. Wu, R. Jia, and C. Liu, "Modeling and characteristics analysis for a buck-boost converter in pseudo-continuous conduction mode based on fractional calculus," *Math. Problems Eng.*, vol. 2016, pp. 1–11, Feb. 2016.
[15] H. Ahn, "Stability and stabilization of fractional-order linear systems subject to input saturation," *IEEE Trans. Autom. Control*, vol. 58, no. 4, pp. 1062–1067, Apr. 2013.
[16] T.-S. Lee and J.-H. Liu, "Modeling and control of a three-phase four-switch PWM voltage-source rectifier in d-q synchronous frame," *IEEE Trans. Power Electron.*, vol. 26, no. 9, pp. 2476–2489, Sep. 2011.
[17] R. Wu, S. B. Dewan, and G. R. Slemon, "Analysis of an AC-to-DC voltage source converter using PWM with phase and amplitude control," *IEEE Trans. Ind. Appl.*, vol. 27, no. 2, pp. 355–364, Mar./Apr. 1991.
[18] A. Davoudi, J. Jatskevich, and T. D. Rybel, "Numerical state-space average-value modeling of PWM DC–DC converters operating in DCM and CCM," *IEEE Trans. Power Electron.*, vol. 21, no. 4, pp. 1003–1012, Jul. 2006.
[19] D. C. Jones and R. W. Erickson, "A nonlinear state machine for dead zone avoidance and mitigation in a synchronous noninverting buck–boost converter," *IEEE Trans. Power Electron.*, vol. 28, no. 1, pp. 467–480, Jan. 2013.
[20] N. R. Tummuru, M. K. Mishra, and S. Srinivas, "Multifunctional VSC controlled microgrid using instantaneous symmetrical components theory," *IEEE Trans. Sustain. Energy*, vol. 5, no. 1, pp. 313–322, Jan. 2014.
[21] M. Sharma and B. S. Rajpurohit, "Investigation of power quality in power distribution system using real-time simulator," in *Proc. 8th IEEE India Int. Conf. Power Electron. (IICPE)*, Jaipur, India, Dec. 2018, pp. 1–6.

MONIKA SHARMA (Member, IEEE) received the M.Tech. degree in electronics and communication engineering from Punjabi University Patiala, Punjab, India, in 2015. She is currently pursuing the Ph.D. degree in investigation on improving power quality in smart grid using voltage source converters with the Indian Institute of Technology Mandi, Mandi, India. Her research interests include power quality, smart grid, wireless sensor networks, signal processing, and smart grid communication.

BHARAT SINGH RAJPUROHIT (Senior Member, IEEE) received the M.Tech. degree in power apparatus and electric drives from the Indian Institute of Technology Roorkee, Roorkee, India, in 2005, and the Ph.D. degree in electrical engineering from the Indian Institute of Technology Kanpur, Kanpur, India, in 2010. He is currently an Associate Professor with the School of Computing and Electrical Engineering, Indian Institute of Technology Mandi, Mandi, India. His major research interests include electric drives, renewable energy integration, and intelligent and energy-efficient buildings. He is a member of the International Society for Technology in Education, the Institution of Engineers, India, and the Institution of Electronics and Telecommunication Engineers.

SAMAR AGNIHOTRI (Member, IEEE) received the M.Sc. (Engg.) and Ph.D. degrees in electrical sciences from IISc Bangalore. From 2010 to 2012, he was a Postdoctoral Fellow with the Department of Information Engineering, The Chinese University of Hong Kong. He is currently an Assistant Professor with the School of Computing and Electrical Engineering, IIT Mandi. His research interests include communication and information theory.

AKSHAY KUMAR RATHORE (Senior Member, IEEE) received the M.Tech. degree from the Indian Institute of Technology (BHU), Varanasi, India, in 2003, and the Ph.D. degree from the University of Victoria, Victoria, BC, Canada, in 2008. He had two subsequent postdoctoral research appointments with the University of Wuppertal, Germany, and the University of Illinois at Chicago, Chicago, IL, USA. From November 2010 to February 2016, he was an Assistant Professor with the Department of Electrical and Computer Engineering, National University of Singapore, Singapore. He is currently an Associate Professor with the Department of Electrical and Computer Engineering, Concordia University, Montreal, QC, Canada. He is leading the area of current-fed power electronics and contributed to analysis, design, and development of new classes of such converters. He has authored or coauthored more than 170 research papers in international journals and conferences, including 58 the IEEE TRANSACTIONS. His research interests include current-fed converters and multi-level inverters.